UMass Optoelectronic Lab on 2D Materials

Antenna enhanced graphene THz emitter and detector

Jiayue Tong, Martin Muthee, Shao-Yu Chen, Sigfrid K. Yngvesson and Jun Yan

Department of Physics, Department of Electrical and Computer Engineering, UMass Amherst

Motivation

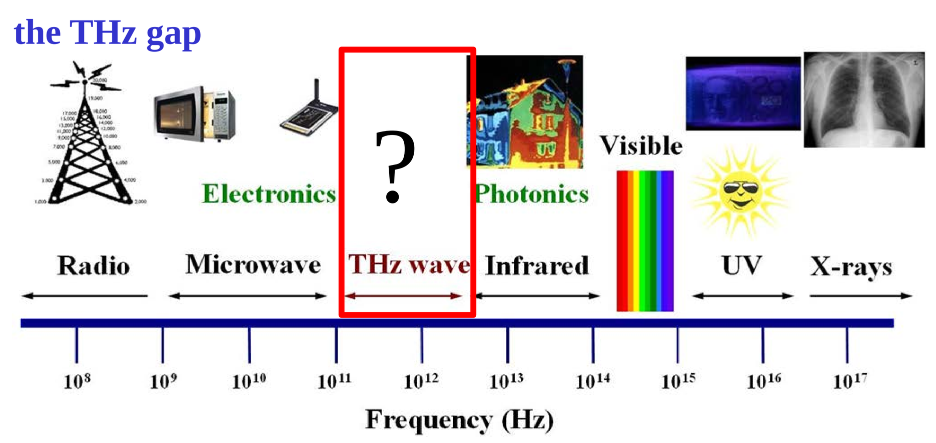

Terahertz radiation, consisting of electromagnetic waves ranging from 0.3 to 10 terahertz (THz), commonly referred to as the terahertz gap, lies in-between the microwaves and infrared light as shown in the picture.

"Terahertz gap" – a region that has been lacking in high performance sources and detectors – is underdeveloped in terms of technology

Graphene: A promising candidate for closing 'THz Gap'

1.Availability: mechanical exfoliation → chemical vapor deposition

*R.S.Ruoff et al. Science **324**, 1312-1314(2009)*

…

2.Tunability: In graphene, the plasmons can be tuned by changing the coupling momentum and carrier density, reaching any frequency from THz to near infrared.

*Feng Wang et al. Nature Nanotechnology **6,** 630-634(2011)*

…

3.Feasibility: Various mechanisms (plasmonic, photovoltaic, bolometric, photon gating …) were proposed and employed for making useful graphene optoelectronic devices

Park et al. Nano Lett. 9, 1742 (2009)

Xia et al. Nature Nanotech. 4, 839 (2009)

Xu et al. Nano Lett. 10, 562 (2010)

Gabor et al. Science 334, 648 (2011)

…

Experiment concept for Graphene THz emitter and detector

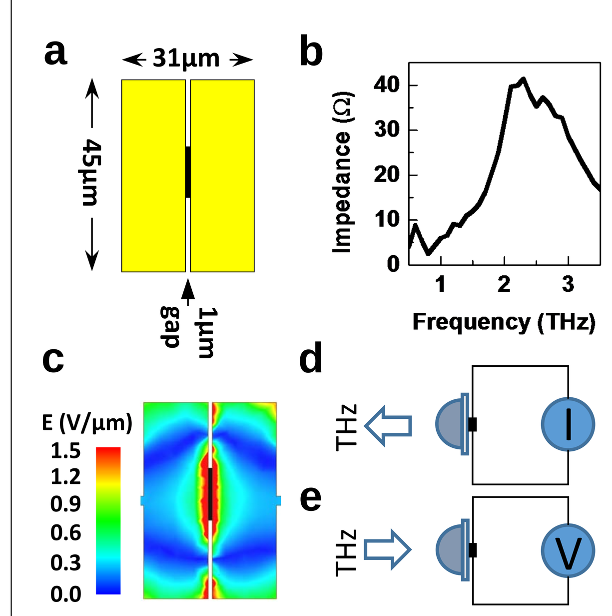

(**a**) Design of the THz antenna coupled graphene device. The graphene piece (black line) is positioned at the center. The 45 μm long slot at the location of the graphene channel is chosen such that it can accommodate well our target frequency at about 2THz (corresponding to a wavelength of 150 μm in free space and 45 μm in silicon).

(**b**) HFSS simulated frequency dependence of impedance.

(**c**) Calculated distribution of THz electric field at 2.1THz.

(**d&e**) Schematic setup of emission (**d**) and detection (**e**) experiments.

Graphene THz emitter fabrication and experimental setup

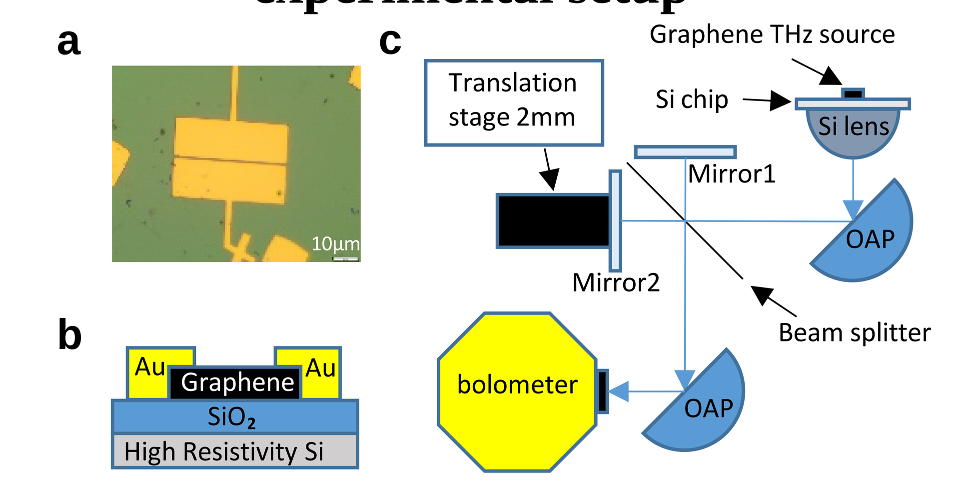

(**a**) Optical image of GFET emitter.

(**b**) Schematic side view of GFET emittier.

(**c**) THz interferometer set up: the collimated light is split by a mylar beam splitter into two arms with the beam paths fixed for one arm and slowly varied for the other. The interference of photons from the two arms is detected by a liquid helium cooled silicon bolometer.

Gate dependence of THz spectrum and THz radiation energy

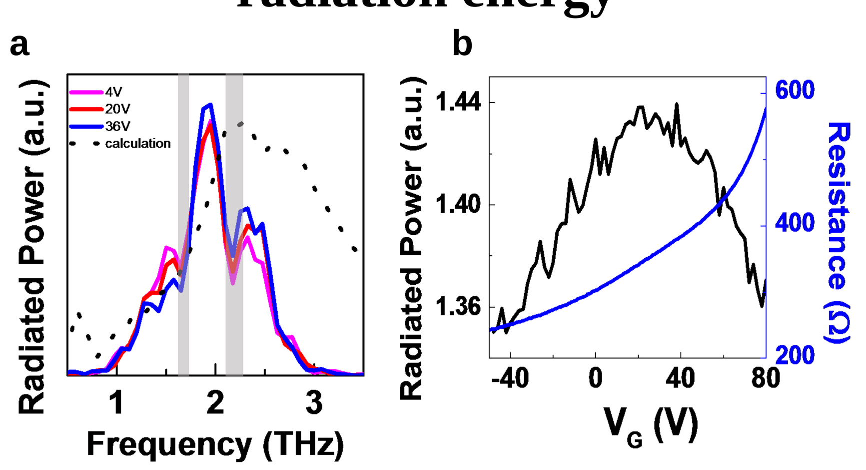

(**a**) Measured (solid lines) THz radiation from graphene at different gate voltages. The dashed line is the transmission spectrum calculated from HFSS simulation. The two grey bands indicate water absorption lines. (**b**) Comparison of V_G dependent GFET resistance (blue) and THz radiated power (black).

DC heating power dependence of graphene temperature and THz radiation energy

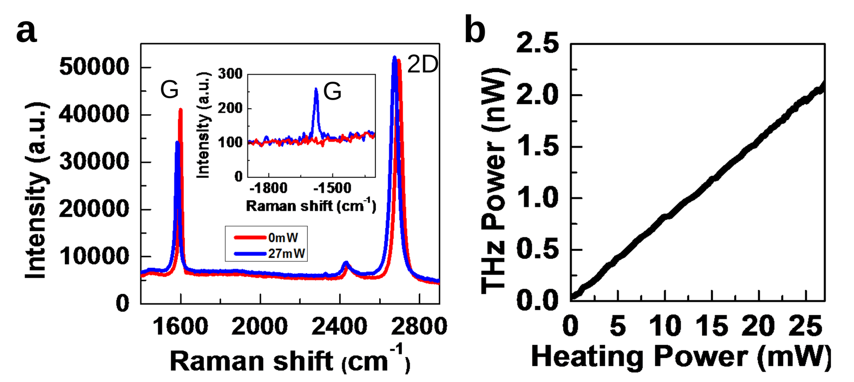

(**a**) Stokes (main panel) and anti-Stokes (inset) Raman spectra of a GFET in the absence (red) and presence (blue) of bias current. The intensity ratio of anti-Stokes and Stokes shows the temperature of graphene reaches 440 ºC with 27mW heating power. (**b**) Dependence of THz radiated power measured by Golay cell on DC electrical heating.

THz detector with edge contacted graphene

THz detection mechanism: The absorption heats up electrons and diffusion of hot carriers establishes in the device a temperature gradient ∇T. This creates a thermoelectric field $E = -S\nabla T$ where S is the Seebeck coefficient. The voltage that we measure is given by a line integration of the electric field along the device between the source and drain electrodes which serve as heat sinks. It is apparent that the detected V would approach zero if E near the source and drain electrodes were to have similar magnitude and opposite signs, so we must break the source-drain mirror symmetry.

Maximizing asymmetry in contacts

a.Fabricating asymmetric contacts on graphene. In our work, we use **edge** contact contact for one side and top contact for the other.

b.Depositing different metals on the two contacts.

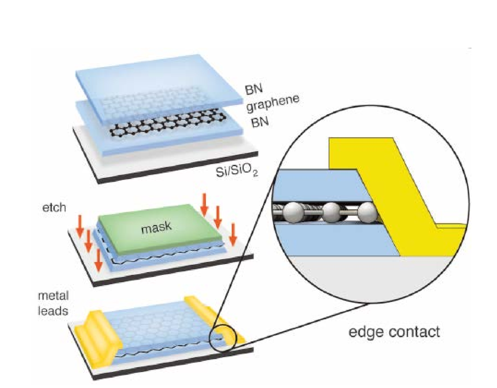

*L.Wang et al. Science **342**, 614(2013)*

Graphene THz detector fabrication and experimental setup

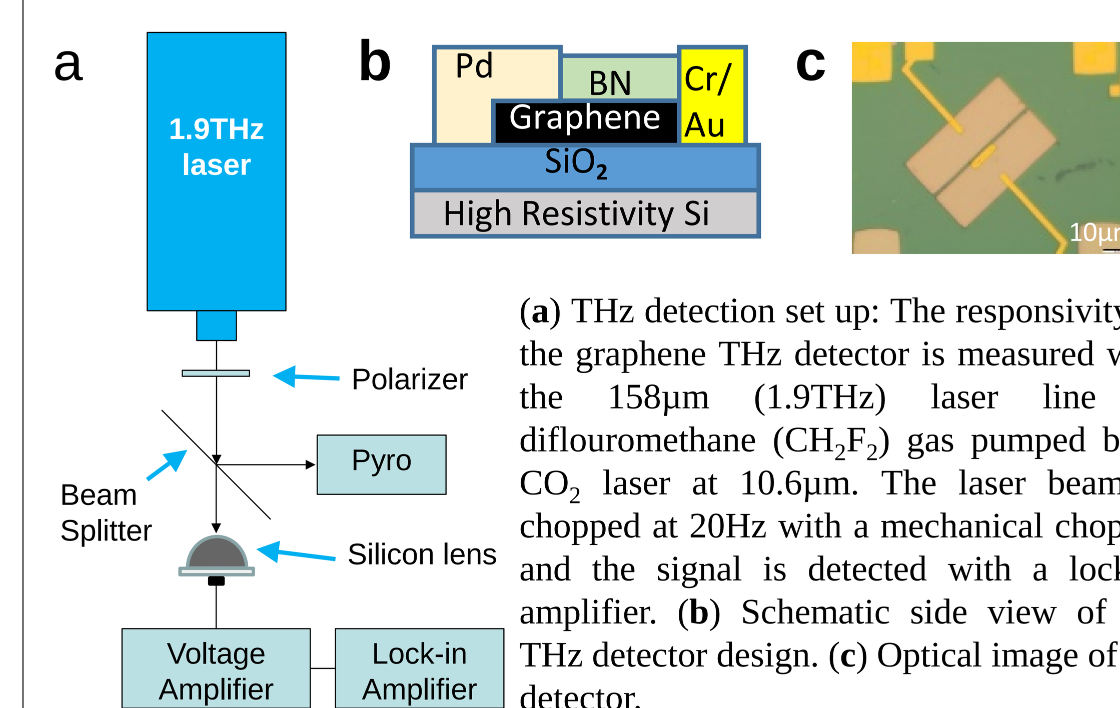

(**a**) THz detection set up: The responsivity of the graphene THz detector is measured with the 158μm (1.9THz) laser line of diflouromethane (CH_2F_2) gas pumped by a CO_2 laser at 10.6μm. The laser beam is chopped at 20Hz with a mechanical chopper and the signal is detected with a lock-in amplifier. (**b**) Schematic side view of the THz detector design. (**c**) Optical image of the detector.

Polarization dependence of normalized THz responsivity

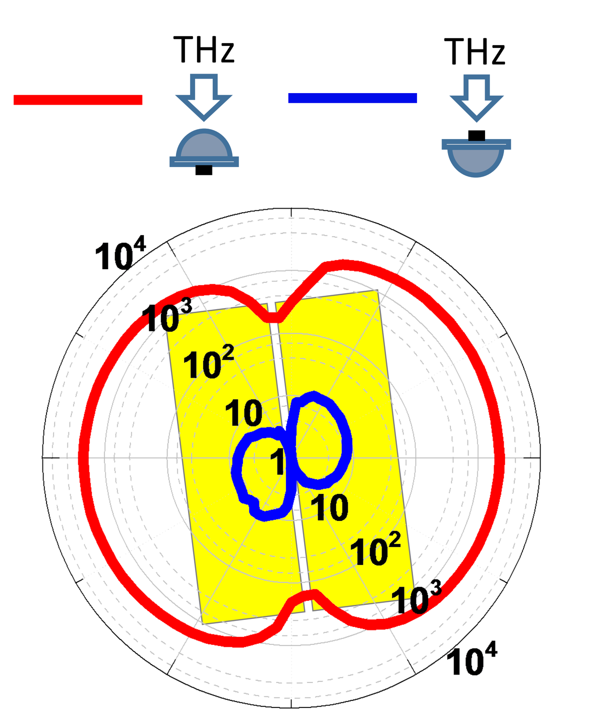

The responsivity is the smallest when the THz light is directly illuminating the antenna and graphene (back illumination, blue curve) with the electric field parallel to the slot. The signal is enhanced by a factor of 2200 when we illuminate through the silicon lens (front illumination, red curve) and align the THz electric field perpendicular to the slot.

Gate dependence of resistance and responsivity

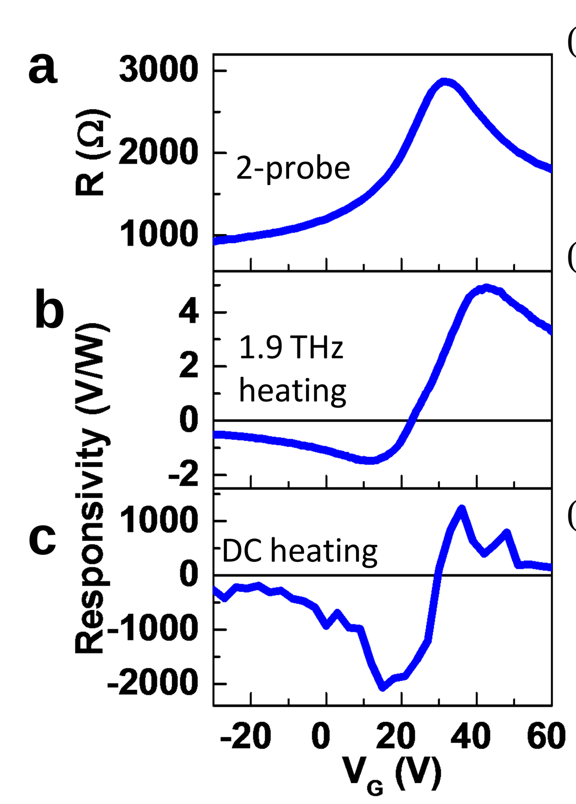

(**a**) The device resistance is measured with a lock-in amplifier (10nA current excitation). The DC gate voltage is varied by a Keithley 2400 multimeter.

(**b**) We measure simultaneously responses from the graphene detector and a commercial pyroelectric detector to normalize the device response to the incident laser power in-situ.

(**c**) A DC bias voltage is used to heat the sample and the thermoelectric current is detected by comparing the magnitude of the electric currents under forward and reverse bias voltages.

Johnson-Nyquist noise and NEP

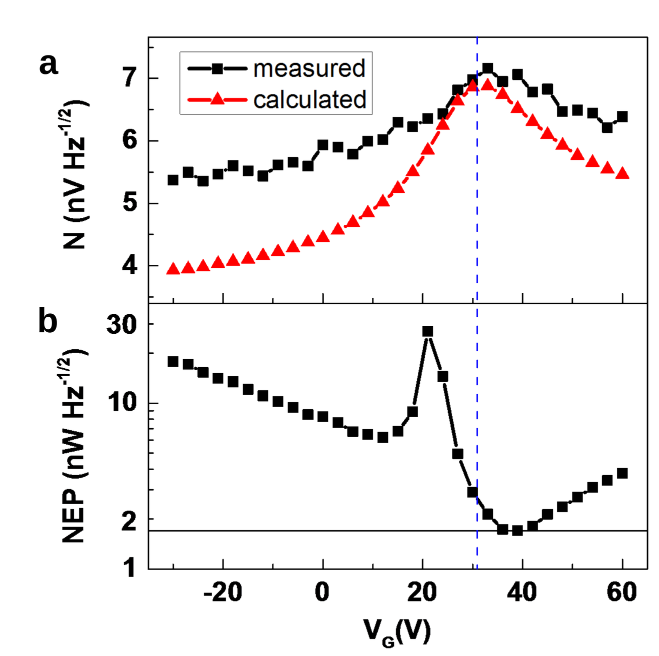

(**a**) Measured noise (black dots) and calculated Johnson-Nyquist noise (red dots) from the equation.

$$V = \sqrt{4k_B TR}$$

(**b**) The NEP of the detector is calculated from the ratio of the noise voltage and the optical voltage responsivity. The NEP reaches a minimum level of 1.7nW·Hz$^{-1/2}$ at the peak responsivity.

Conclusion

We have studied an integrated silicon lens-antenna-graphene transistor system both as emitters and as detectors in the technologically important few THz spectral range. In both applications significant performance improvements are observed due to the enhanced coupling. Our first demonstration of graphene THz emission opens up new opportunities to further investigate plasmon enhanced graphene THz radiation and to create highly efficient and coherent THz light sources. The versatile measurements of the thermoelectric detector delineate in detail how each factor in the design impacts the overall response of the device in a quantitative manner, and pave way for engineering and optimizing each contributing factor leading to commercial graphene THz detectors.

Yan Lab @ Umass Amherst